

Ice Core Records of Atmospheric CO₂ Around the Last Three Glacial Terminations

Hubertus Fischer, Martin Wahlen, Jesse Smith,
Derek Mastroianni, Bruce Deck

Air trapped in bubbles in polar ice cores constitutes an archive for the reconstruction of the global carbon cycle and the relation between greenhouse gases and climate in the past. High-resolution records from Antarctic ice cores show that carbon dioxide concentrations increased by 80 to 100 parts per million by volume 600 ± 400 years after the warming of the last three deglaciations. Despite strongly decreasing temperatures, high carbon dioxide concentrations can be sustained for thousands of years during glaciations; the size of this phase lag is probably connected to the duration of the preceding warm period, which controls the change in land ice coverage and the buildup of the terrestrial biosphere.

Previous studies of Antarctic ice cores (1–3) revealed that atmospheric CO₂ concentrations changed by 80 to 100 parts per million by volume (ppmv) during the last climatic cycle and showed, together with continuous atmospheric measurements (4), that anthropogenic emissions increased CO₂ concentrations from 280 ppmv during preindustrial times to more than 360 ppmv at present, an increase of more than 80% of the glacial-interglacial change. Variations in atmospheric CO₂ concentrations accompanying glacial-interglacial transitions have been attributed to climate-induced changes in the global carbon cycle (5, 6), but they also amplify climate variations by the accompanying greenhouse effect. Accordingly, the relation of temperature and greenhouse gases in the past derived from ice core records has been used to estimate the sensitivity of climate to changes in greenhouse gas concentrations (7) to constrain the prediction of an anthropogenic global warming. This procedure, however, requires the separation of systematic variations representative for all climatic cycles from those specific for each event, as well as a more detailed knowledge of the leads and lags between greenhouse gas concentrations and climate proxies.

To resolve short-term changes in the atmospheric carbon reservoir, to constrain the onset and end of major variations in CO₂ concentrations, and to test whether these variations are temporally representative, we expanded the Antarctic Vostok CO₂ record over the transition from marine isotope stage (MIS) 8 to MIS 7 [about 210 to 250 thousand years (ky) before present (B.P.)] and analyzed the time interval around the penulti-

mate deglaciation (about 70 to 160 ky B.P.) at a high resolution of 100 to 2000 years (8). This data set was supplemented by a CO₂ record recently derived from the Antarctic Taylor Dome (TD) ice core (6, 9) covering the last 35,000 years. The internal temporal resolution of ice core air samples is restricted by the age distribution of the bubbles caused by the enclosure process (10). This age spread is about 300 years for Vostok (11) and 140 years for the TD ice core (9) at present but about three times higher for glacial conditions (11). The depth–ice age scale used for terminations II and III in the Vostok core is a recently expanded version of the extended glaciological time scale (12). The dating uncertainty (on the order of 10,000 years for termination III) is considerable; however, the absolute time scale is not so important as long as we consistently compare Vostok CO₂ with the Vostok isotope temperature (δD) record.

More important is the relative dating of ice and air at a certain depth. The ice age–air age difference (Δage) was calculated with a climatological firn densification model (11) and varies between about 2000 and 6000 years for warm and cold periods, respectively. The accuracy of the model is better than 100 years for recent periods but on the order of 1000 years for glacial conditions (11), which has to be kept in mind when interpreting the phase shift between ice and gas records of the ice core archive. In the case of termination I, recently published age scales derived by synchronization of CH₄ variations in central Greenland and Antarctic ice cores (13, 14) were used. The precision of the CH₄ correlation is about 200 years for periods of substantial CH₄ change but is not very well constrained in the interval between 17 and 25 ky B.P., when only subtle CH₄ changes occurred. The uncertainty of Δage varies between 100 and 300 years for central Green-

land (13) and between 300 and 600 years for TD (14) during termination I. Further uncertainty is added because the TD CO₂ record has been dated relative to the Greenland Ice Sheet Project 2 (GISP2) core (14), whereas the Byrd and Vostok isotope temperature records have been synchronized with respect to the Greenland Ice Core Project (GRIP) ice core record (13). This uncertainty is not relevant for the interval between 10 and 15 ky B.P., for which dating of GISP2 and GRIP is in good agreement; however, there is a shift of up to 2000 years between the two Greenland reference cores at the age of 20 ky B.P.

In Fig. 1, our data and previously published CO₂ concentration records (1, 6, 9, 11, 15, 16) are compared with Antarctic isotope (temperature) ice core records (13, 17–19). Note that the CO₂ concentrations represent essentially a global signal. In contrast, the geographical representativeness of isotope temperature records may vary from a synoptical to hemispherical scale and accordingly within different cores with increasing variability for shorter time scales. The Vostok and TD CO₂ data presented here are in good agreement with previous CO₂ values. On a 10,000-year time scale, CO₂ covaries with the isotope temperatures with minimum glacial CO₂ concentrations of 180 to 200 ppmv, glacial-interglacial transitions accompanied by a rapid increase in CO₂ concentrations to a maximum of 270 to 300 ppmv, and a gradual return to low CO₂ values during glaci-ation. On a shorter time scale, however, a much more complex picture evolves.

The onset of the atmospheric CO₂ increase during termination I recorded in the TD record is at 19 to 20 ky B.P. The rise in the long-term trend in CO₂ concentrations seems to be about 1000 years earlier than the rise in Vostok δD values. In contrast, temperatures apparently started to rise at 20 ky B.P., as recorded in the Antarctic Byrd and the Greenland GRIP ice core (13). Again, CO₂ concentrations in the Byrd record increase ~2000 ± 500 years later than those in the TD data. In view of the excellent agreement for the rest of the CO₂ records, these discrepancies can be attributed to the insufficient age constraint during the onset of termination I induced by the different Greenland reference cores. No such dating uncertainties are encountered for the interval between 10 and 15 ky B.P. Maximum CO₂ concentrations of 270 ppmv are reached at 10.5 ky B.P. (9), 600 to 1000 years after the isotope temperature maximum in the Byrd record (20). The CO₂ peak is followed by a decrease of 5 to 10 ppmv until 8 ky B.P., after which CO₂ concentrations gradually rise to the preindustrial value of 280 ppmv (9). A delay in the increase of CO₂ concentrations with respect to the warming during deglaciation is also indicated by a brief 10-ppmv decline in CO₂ concentrations

Scripps Institution of Oceanography, Geosciences Research Division, University of California San Diego, La Jolla, CA 92093-0220, USA.

REPORTS

found in seven samples during the interval 14 to 13 ky B.P. This distinct feature lags the Antarctic Cold Reversal (ACR) in the Antarctic isotope temperatures (21) by 300 to 500 years but occurs 1000 years before the Younger Dryas cooling event.

A dip in CO₂ concentrations at 135 ky B.P. precedes the start of the increase in CO₂ concentrations during termination II, which reaches a maximum of 290 ppmv at 128 ky B.P. Like in the Holocene, CO₂ concentrations decrease after this initial maximum to ~275 ppmv. The onset of the major warming during termination II is hard to define, but during the penultimate warm period, CO₂ concentrations reach their maximum 400 ± 200 years later than Antarctic temperatures. In the following 15,000 years of the Eemian warm period, CO₂ concentrations do not show a substantial change despite distinct cooling over the Antarctic ice sheet. Not until 6000 years after the major cooling in MIS 5.4 does a substantial decline in CO₂ concentration occur. Another 4000 to 6000 years is required to return to an approximate in-phase relation of CO₂ with the temperature variations.

Finally, termination III starts with a CO₂ concentration of 205 ppmv at 244 ky B.P., slightly higher than that for the beginnings of terminations I and II. At that time, temperatures had already increased since the glacial temperature minimum at ~260 ky B.P. CO₂ concentrations rise slowly from 244 to 241 ky B.P. and then rapidly to more than 300 ppmv at 238 ky B.P. Keeping the rather coarse resolution of the δD record before 238 ky B.P. in mind, the major increase in CO₂ tends to lag temperature during the transition, reaching a maximum CO₂ concentration 600 ± 200 years after the peak in δD. In contrast to the case for the Eemian, high CO₂ concentrations are not sustained during MIS 7 but follow the rapid temperature drop into MIS 7.4. Minimum CO₂ concentrations as low as 210 ppmv are reached 1000 to 2000 years after the minima in isotope temperature during MIS 7.4. A short, warm event during the mild glacial interval at 224 to 228 ky B.P. appears to be reflected in a 30-ppmv increase in atmospheric CO₂ concentrations with a phase lag of about 1000 ± 600 years relative to temperature. Another warm event at the beginning of the warm period MIS 7.3 is accompanied by a 30-ppmv increase in CO₂ concentration, which appears to be in phase with the temperature record. The variations in CO₂ concentrations during these events are much larger than anticipated from the Vostok isotope temperature changes and do not have any counterparts during MIS 5.

Comparison of the sequence of events for the three time intervals described above suggests that the carbon cycle-climate relation should be separated into (at least) a deglaciation and a glaci-ation mode. Atmospheric CO₂ concentrations show a similar increase for all

three terminations, connected to a climate-driven net transfer of carbon from the ocean to the atmosphere (6). The time lag of the rise in CO₂ concentrations with respect to temperature change is on the order of 400 to 1000 years during all three glacial-interglacial transitions. Considering the uncertainties in Δage (between 100 and 1000 years for recent and glacial conditions), such a lag can still be explained by an overestimation of Δage for glacial conditions. The good agreement of the Δage model with the measured value for the present supports the idea that at least the lag at the beginning of the warm periods is real. The size of this lag is on the order of the ocean mixing time (for a well-ventilated ocean like today), which is the major control for the time constant of equilibration within the deep ocean-atmosphere carbon system after climate-induced changes. In the case of a recent anthropogenic warming, the exter-

nal climate forcing by CO₂ emissions due to combustion of fossil fuel leads climate variations, so the application of the CO₂-climate relation deduced from the past on a recent global warming seems not to be straightforward.

The situation is even more complicated for the interglacial and glaci-ation periods. During the extended Holocene and Eemian warm periods, atmospheric CO₂ concentrations drop by ~10 ppmv after an initial maximum, attributable to a substantial increase in the terrestrial biospheric carbon storage extracting CO₂ from the atmosphere. In the case of the Eemian, CO₂ concentrations remain constant after the initial maximum in MIS 5.5 despite slowly decreasing temperatures; during the Holocene, atmospheric CO₂ concentrations even increase during the last 8000 years. Application of a carbon cycle model to CO₂ and δ¹³C₂ ice core data for the Holo-

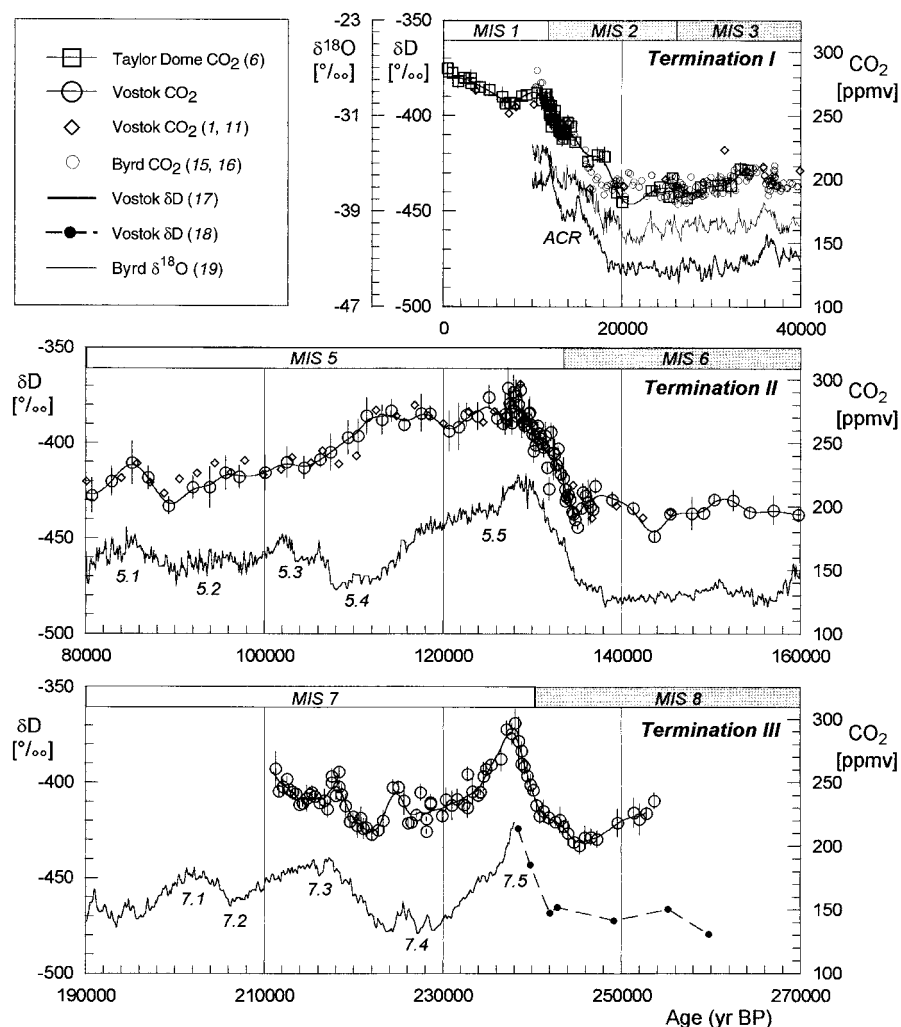


Fig. 1. Records of atmospheric CO₂ concentrations and isotope temperature records derived from the Antarctic Byrd, Vostok, and TD ice cores during the deglaciation and glaci-ation events around the last three glacial terminations. Error bars in CO₂ concentration data represent 1σ of replicate measurements at the same depth interval. The long-term trend in CO₂ concentrations is indicated by a cubic spline approximation ($P = 5 \times 10^{-9}$) of our data set. For convenience, marine isotope stages (22) are indicated as referred to in the text.

cene (9) shows that no equilibrium in the carbon cycle is established and that the waxing and waning of the terrestrial biosphere, possibly related to subtle climate variations and early human land use, are the most important factors controlling atmospheric CO₂ concentrations over the last 10,000 years.

During further glaciation in MIS 5.4, CO₂ concentrations remain constant, although temperatures strongly decline. We suggest that this reflects the combination of the increased oceanic uptake of CO₂ expected for colder climate conditions and CO₂ release caused by the net decline of the terrestrial biosphere during the glaciation and possibly by respiration of organic carbon deposited on increasingly exposed shelf areas. These processes, however, should terminate (with some delay) after the lowest temperatures are reached in MIS 5.4 and ice volume is at its maximum at 111 ky B.P. (22). In agreement with this hypothesis, CO₂ concentrations start to decrease in the Vostok record at about 111 ky B.P. Another possibility to explain this delayed response of CO₂ to the cooling during MIS 5.4 would be an inhibited uptake of CO₂ by the ocean. In any case, about 5°C lower temperatures on the Antarctic ice sheet during MIS 5.4 (17) are difficult to reconcile with the full interglacial CO₂ forcing encountered at the beginning of this cold period and again question the straightforward application of the past CO₂-climate relation to the recent anthropogenic warming.

Another scenario is encountered during MIS 7, in which no prolonged warm period is observed. Although temperatures at the end of termination III are comparable to those at the end of termination II and CO₂ concentrations are even slightly higher, a much shorter lag in the decrease of CO₂ relative to the Antarctic temperature decrease in MIS 7.4 is found. Comparison with the SPECMAP record (23) shows that during the preceding interglacial MIS 7.5, ice volume was much larger than during the Holocene and the Eemian warm periods. Accordingly, the buildup of the terrestrial biosphere during MIS 7.5 is expected to be much less and sea level changes smaller, leading to a smaller net release of CO₂ into the atmosphere during the following glaciation, which is not able to fully counterbalance the CO₂ uptake by the ocean.

References and Notes

1. J. M. Barnola, D. Raynaud, Y. S. Korotkevich, C. Lorius, *Nature* **329**, 408 (1987).
2. A. Neftel, E. Moor, H. Oeschger, B. Stauffer, *ibid.* **315**, 45 (1985).
3. D. Raynaud *et al.*, *Science* **259**, 926 (1993). Recent investigations in central Greenland have reported an *in situ* production of CO₂ in the ice, possibly related to carbonate or organic species reactions (or both), and have strongly compromised the validity of the determined CO₂ concentrations. However, Antarctic ice cores are (if at all) much less affected by this effect because of the very low abundance of reactive carbon species dissolved in Antarctic ice.

4. C. D. Keeling, T. P. Whorf, M. Wahlen, J. van der Plicht, *Nature* **375**, 666 (1995).
5. M. Leuenberger, U. Siegenthaler, C. C. Langway, *ibid.* **357**, 488 (1992).
6. H. J. Smith, H. Fischer, M. Wahlen, D. Mastroianni, B. Deck, in preparation.
7. C. Lorius, J. Jouzel, D. Raynaud, J. Hansen, H. Le Treut, *Nature* **347**, 139 (1990).
8. M. Wahlen, D. Allen, B. Deck, A. Herchenroder, *Geophys. Res. Lett.* **18**, 1457 (1991). Air samples were extracted from Vostok 5G and TD ice with a dry extraction technique, and CO₂ concentrations were determined with laser spectroscopy. The accuracy of a single measurement (as essentially determined by the standard deviation of multiple frequency tunings of the diode laser) is better than 5 ppmv. The laser spectroscopic method enables the use of very small samples (~4 g), allowing us to pick crack-free ice and to measure replicate samples at the same depth interval. In general, all given CO₂ concentrations correspond to the average and standard deviation of at least three replicate samples. On average, the variability of such replicate measurements is 7.5 ppmv (1σ).
9. A. Indermühle *et al.*, *Nature*, in press.
10. J. Schwander *et al.*, *J. Geophys. Res.* **98**, 2831 (1993).
11. J.-M. Barnola, P. Pimienta, D. Raynaud, Y. S. Korotkevich, *Tellus Ser. B* **43**, 83 (1991).
12. Expanded ice age and air age time scales were kindly provided by J. Jouzel and J.-R. Petit. Ages were assigned to sample depths after slight depth corrections for the Vostok 5G core (17) by linear interpolation of the depth-age scale. A publication describing the calculation of the expanded time scales, which is essentially based on the procedure described by J. Jouzel *et al.* [*Nature* **364**, 407 (1993)], is in preparation.
13. T. Blunier *et al.*, *Nature* **394**, 739 (1998).
14. E. J. Steig *et al.*, *Science* **282**, 92 (1998).
15. A. Neftel, H. Oeschger, T. Staffelbach, B. Stauffer, *Nature* **331**, 609 (1988).
16. B. Stauffer *et al.*, *ibid.* **392**, 59 (1998).
17. J. Jouzel *et al.*, *Clim. Dyn.* **12**, 513 (1996).
18. J. R. Petit *et al.*, *Nature* **387**, 359 (1997).
19. S. J. Johnsen, W. Dansgaard, H. B. Clausen, C. C. Langway Jr., *ibid.* **235**, 429 (1972).
20. Phase relations were determined by comparison of maxima and minima in the long-term trend of CO₂ concentrations and isotope temperatures as represented by spline approximations. Given errors reflect the uncertainty in the actual positions of the extrema, which are weakly dependent on the degree of smoothing. They do not take into account the uncertainty in Δage. This additional error is treated separately in the discussion of the data.
21. T. Blunier *et al.*, *Geophys. Res. Lett.* **24**, 2683 (1997).
22. D. G. Martinson *et al.*, *Quat. Res.* **27**, 1 (1987).
23. J. Imbrie *et al.*, in *Milankovitch and Climate*, A. Berger *et al.*, Eds. (Reidel, Hingham, MA, 1984), pp. 269–305.
24. We thank J.-M. Barnola and D. Raynaud for helpful comments and for sharing with us their unpublished Vostok CO₂ record of the last four glacial-interglacial cycles during our sample selection process. This study was funded by NSF grants OPP9615292, OPP9196095, and OPP9118534. Financial support of H.F. has been provided by Deutsche Forschungsgemeinschaft.

30 November 1998; accepted 29 January 1999

Present-Day Deformation Across the Basin and Range Province, Western United States

Wayne Thatcher,^{1*} G. R. Foulger,² B. R. Julian,¹ J. Svarc,¹ E. Quilty,¹ G. W. Bawden¹

The distribution of deformation within the Basin and Range province was determined from 1992, 1996, and 1998 surveys of a dense, 800-kilometer-aperture, Global Positioning System network. Internal deformation generally follows the pattern of Holocene fault distribution and is concentrated near the western extremity of the province, with lesser amounts focused near the eastern boundary. Little net deformation occurs across the central 500 kilometers of the network in western Utah and eastern Nevada. Concentration of deformation adjacent to the rigid Sierra Nevada block indicates that external plate-driving forces play an important role in driving deformation, modulating the extensional stress field generated by internal buoyancy forces that are due to lateral density gradients and topography near the province boundaries.

The northern Basin and Range province is an actively deforming intracontinental plateau lying between the stable blocks of the Sierra Nevada and the Colorado Plateau (Fig. 1).

¹U.S. Geological Survey, MS/977, Menlo Park, CA 94025, USA. ²Department of Geological Sciences, University of Durham, Science Laboratories, South Road, Durham DH1 3LE, UK.

*To whom correspondence should be addressed. E-mail: thatcher@usgs.gov

The province has extended (increased in area) by about a factor of 2 over the past ~20 million years (1, 2), and extension continues with ongoing seismic activity and slip along numerous faults distributed across a zone ~800 km wide (3–5). Constraints on the internal deformation of the province are limited. Geologic studies delineate regions of Holocene and late Quaternary fault slip (3, 4). Space geodetic measurements broadly define movements across the province (6–8), and